Chemical Engineering Journal 359 (2019) 476–484

Contents lists available at ScienceDirect

Chemical Engineering Journal

journal homepage: www.elsevier.com/locate/cej

Carbon nanotube silica composite hollow fibers impregnated with polyethylenimine for CO_2 capture

Laura Keller[a,b], Burkhard Ohs[a], Lorenz Abduly[a], Matthias Wessling[a,b,*]

[a] RWTH Aachen University, Chemical Process Engineering, Forckenbeckstr. 51, 52074 Aachen, Germany
[b] DWI – Leibniz Institute for Interactive Materials, Forckenbeckstr. 50, 52074 Aachen, Germany

HIGHLIGHTS

- CNT matrix proves to be stable after incorporation of silica particles.
- The solid sorbent achieves high CO_2 uptake.
- Adequate models describe the kinetics and isotherms precisely.
- Isothermal operation is possible due to gastight layer applied on the shell side.
- The proposed hollow fibers can act as a platform for multiple functional particles.

GRAPHICAL ABSTRACT

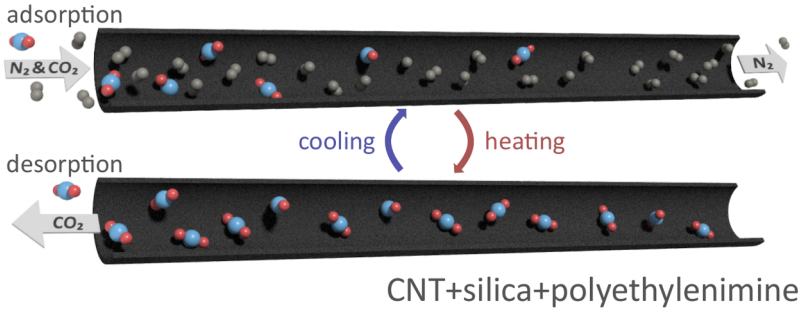

ARTICLE INFO

Keywords:
Hollow fiber sorbents
CNTs
Solid amines
Polyethylenimine
Gas separation
Carbon capture

ABSTRACT

The capture of carbon dioxide from flue gases or air using sorption technologies is an adequate means to stop the increase in CO_2 emissions that are the main contributor to climate change. Hollow fibers for sorption processes are a promising approach with several improved characteristics such as a decreased pressure drop, lower energy consumption as well as higher CO_2 recovery and purity compared to conventional packed-beds. To overcome thermal and chemical limitations of a polymeric matrix we propose carbon nanotube (CNT) based hollow fiber sorbents. Silica particles are dispersed in the CNT network and polyethylenimine is immobilized within the hollow fibers to enhance the sorption performance. Polymeric amines exhibit high CO_2 adsorption capacities even at very low partial pressures. The incorporation of silica particles improves the specific surface area of the so-called microtubes from 203.6 $m^2 g^{-1}$ to 283.2 $m^2 g^{-1}$ and yields a CO_2 uptake of 1.92 mmol g^{-1} at 0.15 bar CO_2 partial pressure. A gas tight polymer layer coated on the shell side allows the use of a thermal moderator for isothermal operation. Adsorption isotherms and kinetics are presented, discussed and fitted applying appropriate models. The results presented here prove the adaptiveness of the carbon nanotube based hollow fibers and emphasize the possibilities they open up as a platform for different sorption tasks that extend beyond carbon capture.

1. Introduction

Anthropogenic greenhouse gas emissions continue to increase and threaten the world's climate [1]. Carbon dioxide makes the largest contribution to these emissions (76%), mostly being emitted from fossil fuel combustion [2]. To mitigate climate change it is imperative to prevent CO_2 from being released into the atmosphere by capturing and storing it [2,3]. So-called carbon capture and storage technologies

* Corresponding author at: RWTH Aachen University, Chemical Process Engineering, Forckenbeckstr. 51, 52074 Aachen, Germany.
E-mail address: Manuscripts.CVT@avt.rwth-aachen.de (M. Wessling).

https://doi.org/10.1016/j.cej.2018.11.100
Received 27 August 2018; Received in revised form 30 October 2018; Accepted 13 November 2018
Available online 15 November 2018
1385-8947/ © 2018 Elsevier B.V. All rights reserved.

could help to achieve the goal of holding the global average temperature below + 2 °C compared to pre-industrial levels and to give humankind enough time to transition from fossil fuels to a society based on renewable energy sources [4].

Adsorption processes are a promising alternative to the energy-intensive amine-based chemical absorption for carbon dioxide separation from flue gas [5] or from ambient air [6]. Research is conducted on a multitude of materials as solid sorbents: zeolites [7,8], metal-organic frameworks [9–11], porous carbons [12,13] or amine-functionalized solid sorbents (e.g., silica [14–16], polymers [17,18], zeolites [19,20], porous carbon [21]). Physisorbents often exhibit low selectivity towards CO_2 and a decrease in adsorption performance under the presence of water vapor [22]. Amine-functionalized solid sorbents, however, can have a number of advantages such as high sorption capacities for CO_2 even at low partial pressures as in air [6], fast ad- and desorption cycles, and low energy consumption [22]. Furthermore, high CO_2 selectivities over N_2 [17,23], CH_4 [24] and O_2 and H_2 [25] have been demonstrated. When humid gas streams are treated sorbents loaded with amines can exhibit increased sorption capacities [26,27] and prove to be stable over multiple ad- and desorption cycles [22].

Carbon nanotubes (CNT) have raised some attention as amine-functionalized sorbents (see Table 1). Several properties render them attractive as a base material to be impregnated with amines: they exhibit high thermal [28] and chemical stability [29]. The excellent thermal conductivity of CNTs [30] may lead to shorter ad- and desorption cycle times in temperature swing adsorption processes. Multiple studies on amine-functionalized carbon nanotubes were conducted in the past. Table 1 gives an overview over the different CNTs and amines that were used as well as the equilibrium CO_2 uptake and the applied temperature and pressure. Promising capacities of up to 3.2 mmol $g^{-1}_{sorbent}$ [31] could be achieved. However, these studies examined amine-functionalized CNTs in powder form which do not allow a direct application. Most adsorption processes take place in packed-bed reactors using beads or granules that are several millimeters in size [32]. These packed-bed columns suffer from different drawbacks such as a significant mass transfer resistance and a high pressure drop at high gas flow rates leading to lower productivity, lower recovery, higher energy requirements as well as gas maldistribution and channelling [33]. Structured adsorbents may overcome the limitations imposed by packed bed adsorption processes [33]. Specifically, hollow fiber sorbents enable a fast mass transfer, offer a significantly reduced pressure drop and more uniform flow conditions [34]. Different approaches to design hollow fiber sorbents have been presented: Feng et al. [34] filled the shell side of a microporous hollow fiber module with sorbent powder (activated carbon or 5A molecular sieve). Using another concept, Lively et al. [35,36] produced polymeric hollow fibers with embedded sorbent particles employing a membrane spinning process. Co-extrusion enabled the formation of a gas-tight layer on the bore side of the fibers which makes rapid heating and cooling as well as isothermal operation possible. Sorbent hollow fibers impregnated with polymeric amines have also been reported [37–40].

In a previously published work, we showed the feasibility and applicability for CO_2 capture of hollow fibers made from carbon nanotubes (CNT) impregnated with polyethylenimine (PEI) [37]. Here, we present hollow fibers made of carbon nanotubes and mesoporous silica particles with improved specific surface area and high carbon dioxide adsorption capacity. Amine-impregnated silica particles are well-studied solid sorbents with promising CO_2 uptake [14–16,38–40,51,52]. Three studies show auspicious results with the same commercially available silica particles [38–40], which were thus used in this work. When integrated into the CNT-based hollow fibers, an adequate framework for gas sorption applications is established. This combines the advantages of thermally, chemically and mechanically stable CNT microtubes with the high CO_2 adsorption capacities of amine-impregnated silica. Furthermore, the cost of the tubular sorbent will be decreased using readily available silica powder. Polyethyleneimine was chosen because its branched chains offer many CO_2 capturing amino groups [53] which yields high CO_2 uptake capacities per molecule [54]. The hybrid hollow fibers were characterized regarding their specific surface area, their mechanical properties were studied, and a gastight layer enabling isothermal adsorption conditions was applied on the shell side of the fibers. A schematic drawing of a hybrid hollow fiber with a gastight neoprene layer on the shell side is presented in Fig. 1a). Fig. 1b) shows multiple of these hollow fibers arranged in a module. The gas flows through the bore side of the fibers while a thermal moderator, e.g. wax, ensures isothermal operation. Furthermore, the CO_2 adsorption behavior is reported and for the adsorption kinetics as well as the isotherms fits are presented using adequate models.

Table 1
Equilibrium capacity of recently developed solid sorbents based on amine-impregnated CNT under dry conditions.

CNT	Amine	Equilibrium CO_2 capacity mmol $g^{-1}_{sorbent}$	CO_2 partial pressure bar	temp. °C	Ref.
SWCNT	linear PEI[1]	2.09	1	27	[41]
MWCNT (OD = 6–9 nm, L = 5 µm)	PEI	2.11	1	25	[37]
MWCNT	PEI	0.35	0.15	40	[42]
MWCNT (ID = 10–20 nm)	linear PEI	1.89	1	70	[43]
MWCNT (L = 10–20 µm)	TEPA[2]	2.97	0.02	25	[44]
MWCNT	TEPA	3.09	0.1	70	[45]
MWCNT	TEPA	3.2	0.1	60	[31]
MWCNT (ID < 10 nm, L = 5-15 µm)	APTES[3]	0.93	0.1	25	[46]
MWCNT	APTES	1.95	0.15	50	[47]
MWCNT	APTES	1.71	0.05	60	[48]
MWCNT (ID = 10–20 nm)	EDA[4]	2.43	1	70	[43]
MWCNT (ID = 5–10 nm)	PDA[5]	0.59	1	30	[49]
MWCNT (OD = 8–15 nm, L = 50 µm)	AEAPS[6]	0.64	0.02	25	[50]

[1] PEI: polyethylenimine.
[2] TEPA: tetraethylenepentamine.
[3] APTES: (3-aminopropyl) triethoxysilane.
[4] EDA: ethylenediamine.
[5] PDA: 1,4-phenylenediamine.
[6] AEAPS: N-(2-aminoethyl)-3-aminopropyltrimethoxysilane.

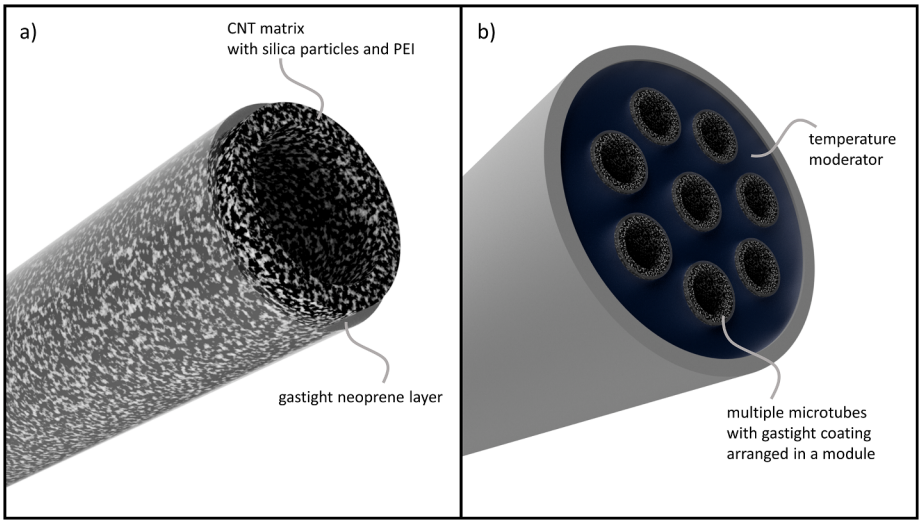

Fig. 1. Schematic drawing of a) a hybrid hollow fiber with a gastight coating on the shell side and b) multiple hollow fibers arranged in a module.

2. Experimental

2.1. Preparation of PEI-impregnated silica CNT hybrid microtubes

The preparation method for pure CNT microtubes has been described before [55]. An aqueous suspension (deionized water, 18 Ω cm) of 1 gL^{-1} multiwalled carbon nanotubes (⩾98% carbon basis, outer diameter: 10 nm ± 1 nm, inner diameter: 4.5 nm ± 0.5 nm, length: 3-6 µm, Sigma Aldrich) and 1 vol% Triton™ X-100 (Sigma Aldrich) was prepared. Different amounts of silica powder (Syloid® C 803, Grace) were added to obtain CNT-silica ratios of 50:50, 30:70, 20:80, and 10:90. The silica powder has a particle size ranging from 3.4 to 4µm and a pore volume of 2 mL g^{-1} [56]. The suspension was magnetically stirred for 30 min and subsequently sonicated for 3 h (UP200S, Hielscher). It was then filtered in inside-out mode through a hollow fiber microfiltration membrane (Accurel PP S6/2, Membrana) of which one end was sealed with adhesive glue. A constant pressure of 5 bar was applied during filtration using a pressure vessel. A carbon nanotube network with embedded silica particles formed on the bore side of the membrane. After the deposition of 6 mg cm^{-2} solids, the fiber was rinsed (inside-out) with 50 mL isopropanol (98% purity, Applichem) at a flow of 0.7 mL min^{-1} using a syringe pump to remove the surfactant. During drying (overnight, 90 mbar vacuum, 30 °C), the CNT network shrinks and the microtube can easily be removed from the hollow fiber membrane.

Polyethylenimine was immobilized on the free-standing microtubes using a common wet impregnation method [57]. PEI (branched, molecular weight: 800 Da, Sigma Aldrich) was dissolved in ethanol (purity > 98.8 vol%, Overlack). The microtubes were suspended in the impregnation solution with either 5 wt% or 20 wt% PEI for 6 h while it was magnetically stirred to ensure a homogeneous immobilization. The impregnation time was chosen after preliminary experiments had revealed that increasing the immobilization time to more than 6 h did not lead to an increase in CO_2 uptake while shorter times resulted in a lower specific CO_2 uptake (see Fig. S1). After the immobilization procedure, the PEI-impregnated microtubes were dried under vacuum (30 °C, 90 mbar) overnight. Further drying and degassing steps prior to any analysis were conducted as described below.

A gas-impermeable neoprene (liquid dispersion with 49–51% solids, grade 842A, Denka) layer was coated on the shell side of the microtube. Prior to the dip-coating process, the neoprene dispersion was diluted to 37.5% and 25% solids using deionized water and magnetically stirred for homogenization. One end of the microtube was sealed with adhesive glue to prevent the neoprene from entering the bore side. The microtube was dipped into the neoprene at a constant velocity of 1.5 mm s^{-1}, left to reside in the polymer dispersion for 2 s and then withdrawn with the same velocity. Subsequently, the microtubes were placed in a drying box under a nitrogen atmosphere for 24 h. The nitrogen was humidified by sparging it through deionized water. Subsequently, the samples were dried another 24 h under vacuum (30 °C, 90 mbar).

2.2. Adsorbent characterization

High-resolution images were produced using three different scanning electron microscopes (S-4800, TM3030plus, and SU9000, Hitachi). The weight fractions of CNT and silica in the microtubes were determined using thermogravimetric analysis (TGA STA6000, Perkin Elmer). Microtubes without PEI or a neoprene coating were crushed for a uniform combustion and heated to 700 °C at 10 °C min^{-1} under a flow of 20 mL min^{-1} synthetic air. According to manufacturer's information, the CNT contain less than 2% impurities. Since the lowest loading of silica was 50 wt%, the impurities could account for a maximum error of 1% and were neglected. Thus, it was assumed that the carbon nanotubes combusted while all that remained after the TGA treatment was silica powder. To analyze the mechanical properties of the microtubes, the flexural strength was determined using a four-point bending test (Microtest, Deben). All samples were 30 mm long and tested at room temperature with a testing speed of 1 mm min^{-1}. The maximum bending strength σ_b is calculated using Eq. (1) [58]

$$\sigma_b = \frac{8 \cdot D \cdot (l - l_1) \cdot F}{\pi \cdot (D^4 - d^4)} \quad (1)$$

where F is the force at the time of fracture, l and l_1 the distance between the outer and the inner support bearings, respectively, D and d the outer and inner diameter of the microtube, respectively. The distance between the outer support bearings was 23.1 mm and between the inner support bearings 6.2 mm. The inner and outer diameter of the microtubes were determined via scanning electron microscopy images. The specific BET surface area was determined by nitrogen adsorption at 77 K (ASAP 2020, Micromeritics). Pure nitrogen adsorption for selectivity calculation was measured at ambient temperature. Samples without PEI were degassed at 300 °C and 1.3 µbar for 4 h while PEI-impregnated samples were degassed at 70 °C and 1.3 µbar for 24 h prior to any nitrogen adsorption measurement.

To check the polymer coating for leaks, the microtube (length: 7.5 cm) was glued (2-K Expoxid glue, Sofortfest, Uhu) into an acrylic glass tube (length: 10 cm, outer diameter: 12 mm) that had a gas outlet in the

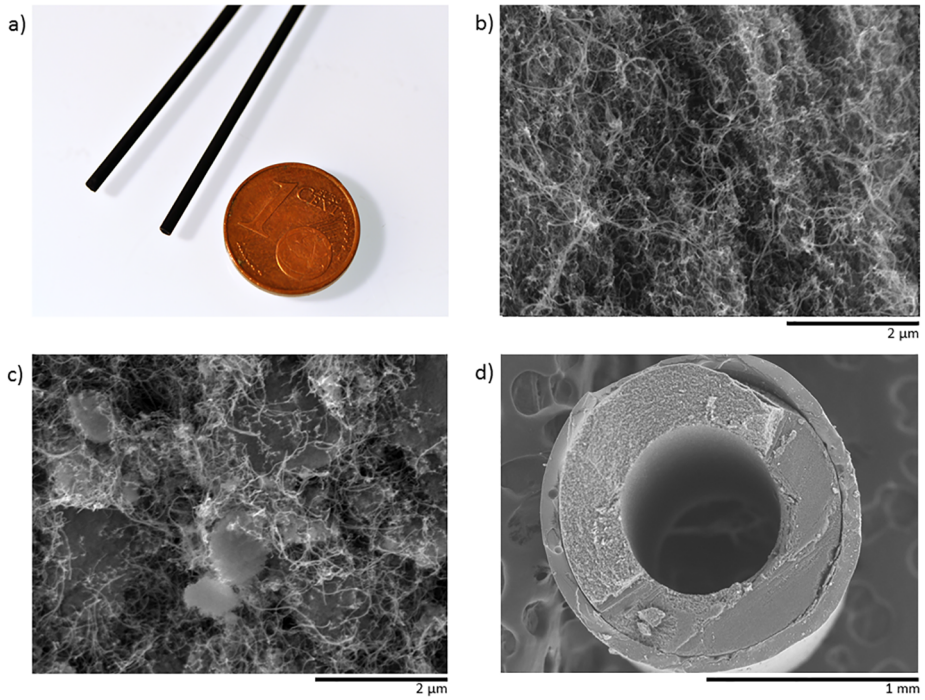

Fig. 2. a) Photo of two microtubes next to a coin for size reference, b) SEM picture of pure CNT microtube, c) SEM picture of microtube with 80 wt% silica, d) SEM picture of a neoprene coated microtube (60 wt% silica, impregnated with PEI: 5 wt% PEI in ethanol).

middle. Two 3D printed spacers at the ends of the microtube ensured radial centering. One side of the microtube was sealed while the other side was used to connect the bore side to pressurized nitrogen. The gas outlet on the shell side allowed to check for gas leakage using a bubble meter. The pressure was increased in steps of 1 bar from 1 to 4 bar, holding each pressure level for 10 min.

2.3. CO_2 adsorption

CO_2 adsorption isotherms were recorded at ambient temperature and at pressures ranging from $3{\cdot}10^{-5}$ to 1.1 bar using pycnometry (ASAP 2020, Micromeritics). Degassing for pycnometry measurements was conducted under vacuum (1.3 µbar) at 70°C for 24 h. The equilibrium criterion was $\frac{p_n - p_{n+1}}{p_n}\frac{1}{\Delta t} < 4.5{\cdot}10^{-7}\frac{1}{s}$ which led to different adsorption times for different samples. Thermogravimetric analysis (TGA STA6000, Perkin Elmer) was used to analyze the kinetics of the carbon dioxide sorption on the PEI-impregnated CNT-silica hybrid hollow fibers and the influence of temperature on the CO_2 uptake. Two different CO_2 concentrations were applied in TGA measurements: 100% and 15 vol% in N_2. To desorb any adsorbed gases and remove water from the sample, a degas step was performed at 110 °C and under nitrogen flow (150 mL min^{-1}) for 120 min. Three adsorption steps under carbon dioxide flow (pure or the gas mixture, 150 mL min^{-1}) were performed at 30 °C, 80 °C, and 110 °C (45 min each). A second desorption step under nitrogen (150 mL min^{-1}, 110 °C, 60 min) was performed after the adsorption step at 30 °C. Subsequently, the adsorption step at 110 °C was performed followed by the adsorption step at 80 °C. An additional adsorption measurement was carried out to determine the CO_2 uptake at 50 °C which is within the temperature range of power plant flue gas [59]. The samples for these TGA measurement were degassed at 110 °C and under nitrogen flow (150 mL min^{-1}) for 120 min. Subsequently, one adsorption step was performed under a flow of 150 mL min^{-1} of a gas mixture (15 vol% CO_2 in nitrogen) at 50 °C for 45 min.

3. Results and discussion

3.1. Adsorbent characterization

The hollow fibers used in this study were prepared via an inside-out filtration method of an aqueous CNT-silica suspension through a commercial microfiltration hollow fiber membrane. The resulting hybrid hollow fibers are shown in Fig. 2a). All microtubes were prepared with a loading of 6 mg_{solid} $cm^{-2}_{membrane}$. The length of the microtube was variable, the wall thickness varied depending on the solid load composition and the outer diameter was approximately 1.35 mm. Scanning electron micrographs visualize the CNT network and the incorporation of silica particles (Fig. 2b)–d)). The network formed by the carbon nanotubes in a hollow fiber without the addition of silica particles can be seen in Fig. 2b). It reveals the intertwining of the CNTs which provides mechanical stability. Additionally, van der Waals forces at points and lines of contact support the cohesion of the network [60]. Fig. 2c) shows the CNT network with embedded silica particles which are incorporated into the network. Images with higher magnification showing the porous structure of the silica particles can be found in the Supporting Information (see Fig. S2). The surrounding carbon nanotubes apparently do not obstruct any of the porosity of the silica. A PEI-impregnated sample is shown in Fig. S2c) and d); however, the PEI film is not optically distinguishable. This indicates that the film is rather thin as thick PEI films on CNT networks manifest themselves in SEM images and can be seen to fill the voids between the CNTs [37]. An impermeable neoprene layer was coated on the shell side of the hollow fiber to enable isothermal adsorption. Fig. 2d) depicts the cross-section of a neoprene-coated hollow fiber with 60 wt% silica and 5 wt% PEI in the impregnation solution. Two different neoprene fractions in the dip-coating solution were tested (25% and 37.5%). The lower concentration yields gastight fibers up to 1.5 bar while the higher concentration proved to form a gastight layer up to a pressure of 4 bar. The layer formed at the higher neoprene concentration has a thickness of 31.7 µm (standard error of the mean of three samples: 2.8). When assembled into a module, a thermal moderator (e.g. wax) can surround the hollow fibers and facilitate isothermal operation [61] while the gas flows

Table 2
Characteristics of the hybrid microtubes: composition measured with TGA, bending strength and corresponding elongation (before PEI impregnation), PEI load on microtube for 5 wt% and 20 wt% PEI in the impregnation solution (number in brackets represents the standard error of the mean). The bending strength of PEI-impregnated hybrid microtubes could not be determined as the fibers did not break.

Silica fraction in suspension wt%	Silica fraction in microtube wt%	Bending strength $N\,mm^{-2}$	Elongation mm	PEI load 5 wt% $g_{PEI}\ g^{-1}_{microtube}$	PEI load 20 wt% $g_{PEI}\ g^{-1}_{microtube}$
0	-	10.6 (0.39)	4.8 (0.83)	0.40 (0.02)	1.26 (0.06)
50	51	4.8 (0.14)	2.4 (0.11)	0.41 (0.04)	–
60	59	5.4 (0.08)	2.5 (0.08)	0.33 (0.01)	1.00 (0.02)
70	65	3.6 (0.13)	1.8 (0.23)	0.43 (0.02)	1.67 (0.06)
80	79	2.5 (0.05)	1.1 (0.05)	0.38 (0.02)	–
90	89	1.3 (0.13)	0.8 (0.01)	–	–

through the bore side of the fibers. Fan et al. [40] reported the importance of heat dissipation and thus isothermal operation when amine-impregnated hollow fibers are used for carbon dioxide adsorption and found that breakthrough capacities increased by 30% when a heat-conducting module was used.

Hybrid hollow fibers with 50, 60, 70, 80, and 90 wt% silica were produced in this study and compared with PEI-impregnated pure CNT hollow fibers. Thermogravimetric analysis was conducted to confirm that the silica fraction within the hybrid hollow fibers was equal to the silica fraction added to the aqueous CNT suspension. The results are presented in Table 2. The largest deviation of 5 wt% was found for 70 wt% silica particles in the silica-CNT suspension. All other samples deviated by 1 wt%. Thus, the fabrication method allows the precise tuning of silica weight fraction in the hybrid hollow fibers. The influence of the silica particles in the CNT matrix on the mechanical stability of the hollow fibers was analyzed using a four-point bending test. As can be seen in Table 2, both the bending strength and corresponding elongation decrease with increasing silica content. The bending strength of a fiber with 90 wt% silica is nearly one order of magnitude lower than the one of a pure CNT hollow fiber. Qualitatively, the fibers with silica were more brittle and broke more suddenly than pure CNT fibers. The decrease in elongation with increasing silica fraction quantitatively supports our observation. Additionally, fibers with 90 wt % silica were too brittle for PEI impregnation and could not be used for carbon dioxide adsorption. Fibers with increasing silica content were, nonetheless, less prone to damage when squeezed, i.e. they resisted irreversible deformation. Impregnating the fibers with PEI improved the mechanical stability significantly. However, this could not be quantified by the four-point bending test as the fibers did not break but were merely bent and pulled through the testing apparatus. Table 2 also shows the PEI load on the microtube after immobilization. It appears that for the low PEI fraction in the impregnation solution, the PEI load on the hollow fiber is independent of the PEI content and lies around 0.4 $g_{PEI}\ g^{-1}_{microtube}$. For the higher PEI fraction in the impregnation solution, an increase from 60 wt% to 70 wt% is observed. More microtubes with different silica fractions need to be impregnated with PEI to confirm this observation for other silica contents.

The specific surface area of the hollow fiber sorbents was determined using nitrogen adsorption at 77 K. All nitrogen adsorption and desorption isotherms can be found in the Supporting Information (Figure S2). As Fig. 3 shows, a linear increase of the specific surface area with an increasing silica weight fraction is observed. The line of best fit for the hybrid hollow fibers almost goes through the values of the specific surface area of the pure starting materials. Thus, the specific surface area of the hybrid microtube depends linearly on the mass fractions of CNTs and silica. Furthermore, this indicates that the CNT matrix does not obstruct the silica particles and their internal surface area is completely available for the amine-impregnation. PEI-impregnated hollow fiber sorbents exhibit a decreased specific surface area compared to the fibers without immobilized PEI which is attributed to the PEI adsorbing to the CNTs and to the silica particles and thus

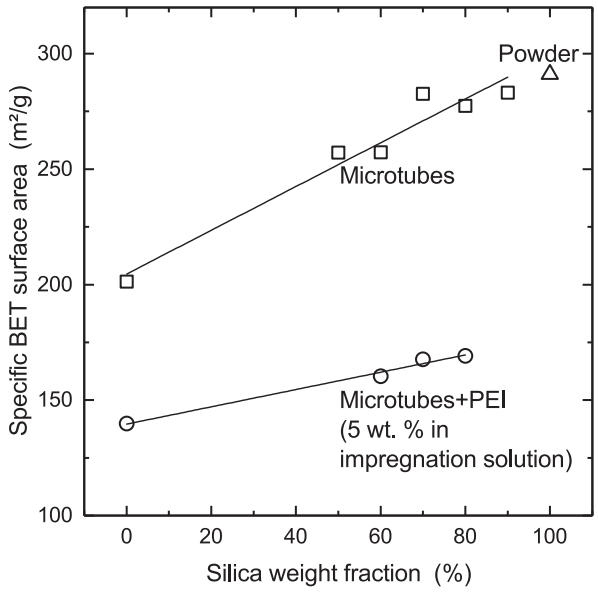

Fig. 3. Specific BET surface area of hybrid microtubes before PEI immobilization and with 5 wt% in the impregnation solution. Lines represent the line of best fit for the microtube data with and without PEI impregnation.

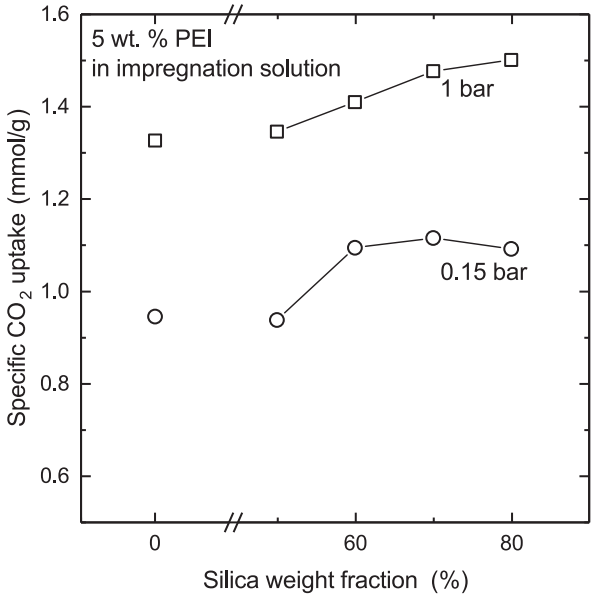

Fig. 4. Specific CO_2 uptake of fibers with different silica weight fraction and 5 wt% PEI in the impregnation solution measured with pycnometry at ambient temperature.

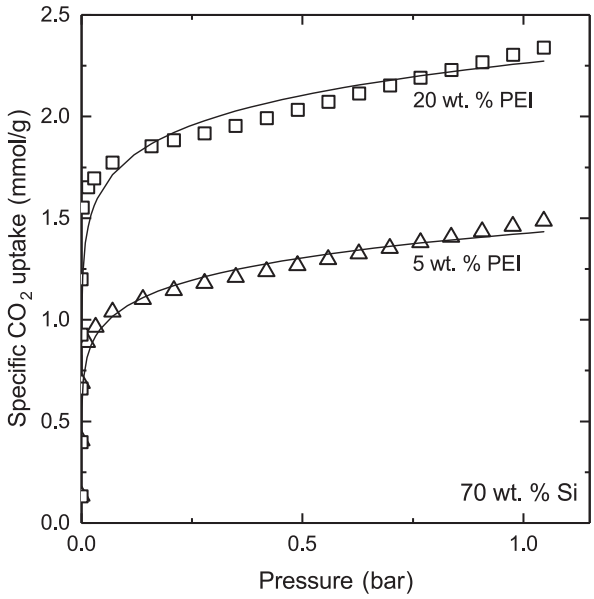

Fig. 5. Adsorption isotherms for fibers with 70 wt% silica from $3{\cdot}10^{-5}$ to 1.1 bar at ambient temperature. Experimental data is represented by the open symbols while the lines represent the fits of the Freundlich model.

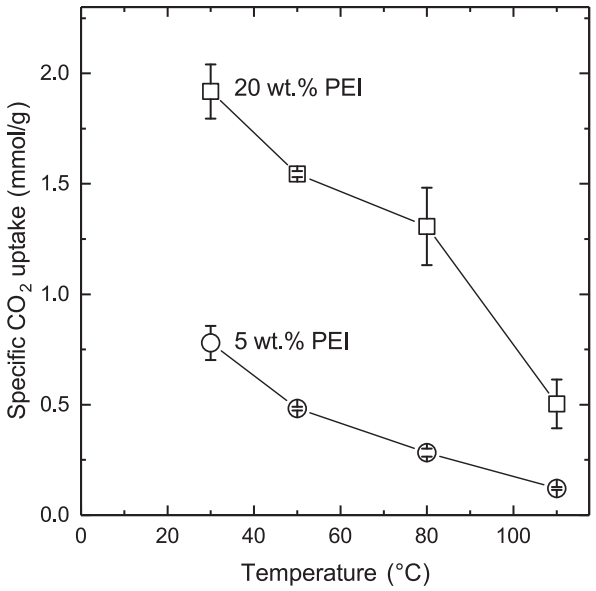

Fig. 6. TGA measurements of specific CO_2 uptake after 45 min at different temperatures and with 15 vol% CO_2 of fibers with 70 wt% silica and 30 wt% CNT impregnated with 5 wt% and 20 wt% PEI in ethanol. Error bars represent the standard error of the mean.

reducing the internal surface area. A linear increase with increasing silica weight fraction can still be observed. The pore size distribution of the hollow fiber sorbents is shown in Fig. S4. The incorporation of silica particles leads to a shift of pore width to smaller values.

3.2. CO_2 adsorption

The carbon dioxide uptake of the PEI-impregnated hollow fibers was measured using pycnometry at ambient temperature and gravimetry (i.e. thermogravimetric analysis) at different temperatures. Two PEI-loadings were tested: 5 wt% and 20 wt% in ethanol. The latter had been found to yield the highest CO_2 uptake on PEI-impregnated CNT hollow fibers [37]. The specific CO_2 uptake at 1 bar and 0.15 bar for fibers with different silica weight fractions and 5 wt% PEI in the impregnation solution is shown in Fig. 4. The lower pressure of 0.15 bar was chosen because it is close to the partial pressure of CO_2 in flue gases [62]. A linear increase in specific CO_2 uptake at 1 bar can be observed with increasing silica weight fraction from 1.3 mmol g^{-1} for a pure CNT hollow fiber to 1.5 mmol g^{-1} for 80 wt% silica. However, the increase from 50 wt% to 80 wt% silica is small (0.15 mmol g^{-1}). At 0.15 bar, an initial increase in CO_2 uptake occurs from 50 wt% to 60 wt%. From 60 wt% to 80 wt% the CO_2 uptake seems to plateau. The minor changes in CO_2 uptake with increasing silica content accord with the constant PEI load at 5 wt% in the impregnation solution.

The pycnometry measurements also provide adsorption isotherms from $3{\cdot}10^{-5}$ bar to 1.1 bar, which are shown in Fig. 5 for the two different PEI-loads on a fiber with 70 wt% silica. The fibers exhibit a steep increase in adsorbed CO_2 up to approximately 0.05 bar to 1.04 mmol g^{-1} and 1.77 mmol g^{-1} for 5 wt% and 20 wt%, respectively, followed by a slow increase to 1.49 mmol g^{-1} and 2.34 mmol g^{-1} at 1.1 bar. Different isothermal models exist to fit the behavior of different sorbents but the Freundlich isothermal model was found adequate to describe the behavior of amine-functionalized sorbents [16]. The Freundlich equation [63]

$$q_e = K_f \cdot p_{CO_2}^{1/n} \tag{2}$$

is an empirical model that can be applied to nonideal sorption on heterogeneous surfaces as well as multilayer sorption [64]. Here, q_e is the amount of CO_2 adsorbed at the partial pressure p_{CO_2} while K_f and n are constants of the model. The behavior of the PEI-impregnated silica CNT hollow fibers is described precisely by the Freundlich model as Fig. 5 and the coefficient of determination R^2 show. The model parameters are summarized in Table 3. The steep increase in CO_2 uptake at very low partial pressures has been observed elsewhere for the adsorption of carbon dioxide on PEI [65] and indicates a good applicability of the PEI-impregnated hybrid hollow fibers for the direct capture of CO_2 from air with a current concentration of 400 ppm [66].

The selectivity of the hybrid hollow fibers for CO_2 over N_2 was determined using pycnometry data collected at ambient temperature for an assumed gas mixture of 15 vol% CO_2 in N_2 at a total pressure of 1 bar. Different works on PEI-impregnated sorbents [17,23,37] calculated the selectivity using the ideal adsorption solution theory [67]

$$S = \frac{q_{CO_2}/q_{N_2}}{p_{CO_2}/p_{N_2}} \tag{3}$$

where the moles of CO_2 adsorbed q_{CO_2} are divided by the moles of N_2 adsorbed q_{N_2} and normalized by the corresponding partial pressures p_{CO_2} and p_{N_2}. A selectivity of 188 was calculated for the hybrid hollow fiber sorbent consisting of 70 wt% silica and impregnated with 5 wt% PEI in the impregnation solution while the same hollow fiber impregnated with 20 wt% PEI in the impregnation solution exhibited a selectivity of 217. An increase in selectivity at increasing PEI contents has also been observed elsewhere [23,17]. The hollow fiber sorbents presented in this work potentially enable selective CO_2 adsorption. More measurements at higher temperatures and with mixed gases will be part of future work.

The measurements of CO_2 uptake using thermogravimetric analysis yield the adsorption kinetics of the hollow fiber sorbent as well as

Table 3
Constants for Freundlich isothermal models. K_f, K_L, and n are model constants, q_{sat} denotes the saturation of adsorbed CO_2 and R^2 is the coefficient of determination.

Parameter	Unit	5 wt%	20 wt%
K_f	mmol g^{-1} Pa^{-1}	1.42	2.26
n	–	7.89	9.58
R^2	–	0.94	0.90

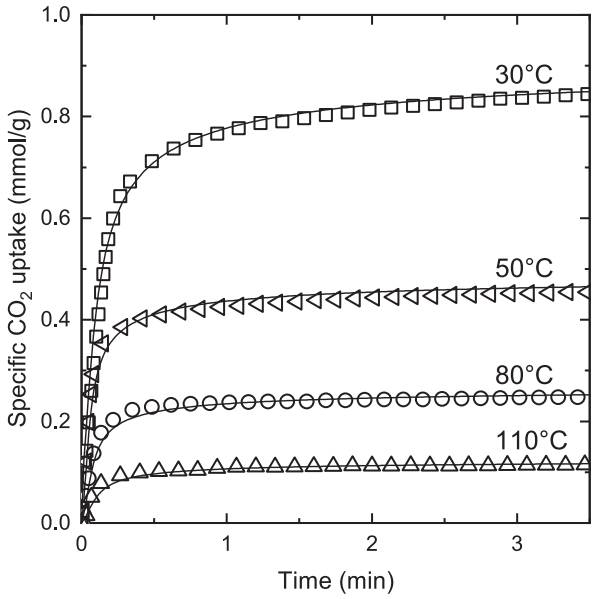

Fig. 7. Adsorption kinetics of a fiber consisting of 70 wt% silica and 30 wt% CNT impregnated with 5 wt% PEI in the impregnation solution. The measurement was performed with thermogravimetric analysis using a gas mixture of 15 vol% CO_2 and 85 vol% N_2. Open symbols represent experimental data while the lines depict the results from the dual kinetic model fit.

Table 4
Values for the dual kinetic model parameters. k_{DKM} is a temperature-dependent kinetic parameter and n_{DKM} a constant of the model while β_{DKM} is the ratio of k_{bulk} and k_{sur} (the kinetic parameters for bulk and surface sorption, respectively). R^2 is the coefficient of determination.

Parameter	Unit	30 °C	50 °C	80 °C	110 °C
k_{DKM}	s^{-1} $mmol^{1-n_{DKM}}$ g^{nDKM-1}	3.69	13.99	77.7	330.01
β_{DKM}	g $mmol^{-1}$	9.79	17.37	36.37	67.83
n_{DKM}	–	3.25	3.25	3.25	3.25
R^2	–	0.99	0.98	0.97	0.95

uptake values at different temperatures. Fig. 6 shows the specific CO_2 uptake of hybrid hollow fibers consisting of 70 wt% silica and 30 wt% CNT impregnated with either 5 wt% or 20 wt% PEI in the impregnation solution at different temperatures. A decrease in CO_2 uptake with increasing temperature can be observed leading to working capacities of 0.66 mmol g^{-1} for 5 wt% PEI in ethanol between 30 °C and 110 °C and 1.41 mmol g^{-1} for 20 wt%. An increase of the PEI fraction in the impregnation solution thus leads to a significant increase both in working capacity and total CO_2 uptake. Previous work has shown an optimum of PEI load on different substrates [37,38,68]. The amount of PEI has thus to be increased carefully not to exceed this optimum.

Fig. 7 shows the specific CO_2 uptake under 15 vol% CO_2 and 85 vol % N_2 over time for a microtube with a silica fraction of 70 wt% silica and impregnated with 5 wt% PEI in the impregnation solution. The adsorption kinetics are representative for other PEI-impregnated hybrid microtubes and can be described using the recently developed dual kinetic model (DKM) which accurately describes the adsorption kinetics of amine-functionalized sorbents [69]. The CO_2 uptake is modeled as a function of a kinetic factor, the adsorption driving force and the current carbon dioxide load [69]

$$\frac{\partial q_t}{\partial t} = k_{DKM}\cdot(1 + \beta_{DKM}\cdot q_t)\cdot(q_{eq} - q_t)^{n_{DKM}} \quad (4)$$

with q_t and q_{eq} representing the equilibrium and the current loading at the time t, respectively, k_{DKM} being a temperature-dependent kinetic parameter and n_{DKM} a constant of the dual kinetic model, and β_{DKM} the ratio of k_{bulk} and k_{sur} (the kinetic parameters for bulk and surface sorption, respectively).The adsorption kinetics of the PEI-impregnated hybrid hollow fibers are precisely described by the dual kinetic model (see Fig.7).The coefficient of determination R^2 being near unity (cf.Table 4) emphasizes the good fit of the DKM. All model parameters are summarized in Table 4.As can be seen in Fig.7, higher temperatures lead to faster kinetics, i.e.at 80 °C and 110 °C the equilibrium uptake is reached more rapidly than at 30 °C. After 3 min, an average of 93.8% (1.4%) and 97.3% (4.7%) of the CO_2 uptake compared to the uptake after 45 min are reached at 80 °C and 110 °C, respectively (values in brackets represent the standard error of the mean of three measurements performed with three different fibers).This indicates short desorption times at elevated temperatures due to fast kinetics.At 30 °C, 78.7% (6.9%) and at 50 °C, 89.7% (0.5%) of the CO_2 uptake are reached after 3 min.The working capacity at this time is 0.50 mmol g^{-1} (between 30 °C and 110 °C), which is lower than the working capacity of 0.66 mmol g^{-1} after 45 min.This results from the difference in kinetics at different temperatures.Nevertheless, short cycle times are feasible but entail a loss in adsorption capacity.Under process conditions, the benefit of short cycle times and thus high throughput have to be carefully weighed against the adsorption capacity.When treating a gas stream at elevated temperatures (i.e.50 °C) as it would be the case for flue gases, a working capacity 0.32 mmol g^{-1} is reached after 3 min which is 88.9% of the working capacity after 45 min (0.36 mmol g^{-1}).Thus, a higher temperature of the treated gas stream leads to decreased working capacities but also benefits from the faster kinetics at higher temperatures.However, not only the ad- and desorption temperatures influence the working capacity, but an interplay of pressure and temperature were found to affect both selectivity and working capacity [70]. Increasing the desorption temperature further could potentially lead to a larger working capacity. However, degeneration of PEI was demonstrated starting at 135 °C [71]. Another option to improve the working capacity is the use of steam, as has been proposed in literature [71,72]. Cyclic measurements under humidified CO_2 with hybrid hollow fibers consisting of 70 wt% silica and impregnated with PEI (20 wt% PEI in the impregnation solution) with and without a neoprene coating on the shell side (neoprene dispersion with 37.5% solids) show an increased uptake of up to 5.1 mmol g^{-1} at 50 °C (see Figs. S5 and S6). The pure CO_2 stream contained 65% relative humidity (8 vol% water) which is realistic for a flue gas stream [73]. How much water is adsorbed under such conditions needs to be investigated. Under the applied conditions the sorbents could fully be regenerated, but a slight decrease of maximum uptake was noticed for each cycle. Without the neoprene coating, a 4% decrease between the first and the last cycle were found while with the neoprene coating, a decrease of CO_2 only started after the second cycle and amounted to 3% between the first and the last cycle. The neoprene coating may help prevent leaching of the PEI but further study of the cyclic behavior of the sorbents is necessary to confirm this observation.

Although both an increase in silica content and a higher PEI fraction in the impregnation solution lead to an increase in CO_2 uptake, the PEI fraction has a stronger influence. This becomes apparent when comparing Fig. 4 and Fig. 6. At a CO_2 partial pressure of 0.15 bar

Table 5
Comparison of CO_2 uptake of a hybrid and a pure CNT hollow fiber at different PEI loads and 0.15 bar CO_2 partial pressure. Values in brackets represent the standard error of the mean.

Silica fraction wt%	PEI fraction in ethanol wt%	CO_2 uptake pycnometry mmol $g^{-1}_{sorbent}$	CO_2 uptake gravimetric mmol $g^{-1}_{sorbent}$
0	5	0.95	1.17 (0.06)
0	20	2.12	1.46 (0.04)
70	5	1.1	0.78 (0.08)
70	20	1.85	1.92 (0.12)

pycnometry revealed an increase from 0.95 mmol g^{-1} for pure CNT microtubes with 5 wt% PEI in the impregnation solution to 1.09 mmol g^{-1} for 80 wt% silica and the same amount of PEI. Increasing the PEI fraction in the impregnation solution from 5 wt% to 20 wt% on the other hand led to an increase in CO_2 uptake on fibers with 70 wt% silica from 1.1 mmol g^{-1} to 1.85 mmol g^{-1} (measured with pycnometry) or from 0.78 mmol g^{-1} to 1.92 mmol g^{-1} (measured with gravimetry). A comparison of pycnometry and gravimetry data for pure as well as hybrid microtubes can be found in Table 5. The pycnometry measurements are single measurements with a different adsorption time than the gravimetric measurements depending on the equilibrium condition described in Section 2.3. These two factors may explain the difference in the results from pycnometry and gravimetric measurements. Overall, Table 5 reveals that there is a slight or no improvement in CO_2 uptake when incorporating silica particles in the CNT microtubes. This evidence is reflected by the unchanged PEI uptake over increasing silica contents for low PEI concentrations (5 wt% in ethanol, see Table 1). It may be favorable to use different silica particles with tailored pore size and surface chemistry, which could improve the PEI loading and more importantly enhance the CO_2 uptake significantly [74]. However, in this work the feasibility of incorporating silica into the CNT-based hollow fibers was proven. No modification of the preparation method is needed. This opens up the possibility to manufacture hybrid microtubes with a multitude of functional materials for different purposes (gas separation but also electrode properties enhanced with e.g. catalyst particles) while conserving the advantages of carbon nanotubes as a base material.

4. Conclusion

Efficient sorption processes require tailored sorbent properties. In this work, the feasibility of producing free-standing hybrid hollow fibers consisting of carbon nanotubes and silica particles was demonstrated which enables the adjustment of the sorbent properties to a specific sorption task. The simple production process offers the possibility of including many other functional particles in the microtubes opening up a multitude of application opportunities. The advantage of the CNT-based material over e.g. polymeric substances is the thermal, chemical and mechanical stability of the CNT. The bending strength of the fibers decreased with increasing silica content from 10.6 N mm^{-2} to 1.3 N mm^{-2} (for 0 and 90 wt% silica, respectively). Impregnating the microtubes with PEI, however, led to an improved elasticity of the microtubes. After PEI-impregnation a gastight layer consisting of neoprene was successfully coated on the shell side of the hollow fibers. This allows the implementation of a temperature-controlled module which enhances the carbon dioxide adsorption capacity in a process. Increasing the silica content leads to an increase in specific surface area to 283.2 $m^2 g^{-1}$ and in CO_2 uptake to 1.1 mmol g^{-1} for 5 wt% PEI in the impregnation solution. Nevertheless, the influence of an increase in PEI load is more pronounced and also leads to an increase in CO_2 uptake to 1.92 mmol g^{-1}. Future research should explore an optimum PEI load for these hybrid hollow fibers. Furthermore, the adsorption capacity of the CNT-silica microtubes should be tested in a module both for direct air capture as well as simulated flue gas.

Acknowledgement

M.W. acknowledges the support through an Alexander-von-Humboldt Professorship. This work was performed in part at the Center for Chemical Polymer Technology CPT, which is supported by the EU and the federal state of North Rhine-Westphalia (Grant No. EFRE 30 00 883 02). The authors thank Robert Sengpiel for proofreading and valuable suggestions, Claudia Pörschke for the TGA measurements as well as Zeynep Aydin for her contributions to the bending strength and specific surface area measurements.

Appendix A. Supplementary data

Supplementary data associated with this article can be found, in the online version, athttps://doi.org/10.1016/j.cej.2018.11.100.

References

[1] T.F. Stocker, Q. Dahe, G.-K. Plattner, L.V. Alexander, S.K. Allen, N.L. Bindoff, F.-M. Bréon, J.A. Church, U. Cubash, S. Emori, P. Forster, P. Friedlingstein, L.D. Talley, D. G. Vaughan, S.-P. Xie, Technical Summary, Climate Change 2013: The Physical Science Basis. Contribution of Working Group I to the Fifth Assessment Report of the Intergovernmental Panel on Climate Change, 2013, 33–115.https://doi.org/10.1017/CBO9781107415324.005.

[2] IPCC, Climate Change 2014: Mitigation of Climate Change. Contribution of Working Group III to the Fifth Assessment Report of the Intergovernmental Panel on Climate Change, Cambridge University Press, Cambridge, UK and New York, NY, USA, 2014.https://doi.org/10.1017/CBO9781107415416.

[3] IEA, 20 years of carbon capture and storage. Accelerating future deployment.

[4] R.S. Haszeldine, Carbon capture and storage: how green can black be? Science (New York, N.Y.) 325 (5948) (2009) 1647–1652, https://doi.org/10.1126/science.1172246.

[5] A. Samanta, A. Zhao, G.K. Shimizu, P. Sarkar, R. Gupta, Post-combustion CO_2 capture using solid sorbents: a review, Ind. Eng. Chem. Res. 51 (4) (2012) 1438–1463, https://doi.org/10.1021/ie200686q.

[6] A. Goeppert, M. Czaun, R.B. May, G.K. Prakash, G.A. Olah, S.R. Narayanan, Carbon dioxide capture from the air using a polyamine based regenerable solid adsorbent, J. Am. Chem. Soc. 133 (50) (2011) 20164–20167, https://doi.org/10.1021/ja2100005.

[7] T.-H. Bae, M.R. Hudson, J.A. Mason, W.L. Queen, J.J. Dutton, K. Sumida, K.J. Micklash, S.S. Kaye, C.M. Brown, J.R. Long, Evaluation of cation-exchanged zeolite adsorbents for post-combustion carbon dioxide capture, Energy Environ. Sci. 6 (1) (2013) 128–138, https://doi.org/10.1039/C2EE23337A.

[8] Z. Liu, C.A. Grande, P. Li, J. Yu, A.E. Rodrigues, Adsorption and desorption of carbon dioxide and nitrogen on zeolite 5A, Sep. Sci. Technol. 46 (3) (2011) 434–451, https://doi.org/10.1080/01496395.2010.513360.

[9] J.A. Mason, K. Sumida, Z.R. Herm, R. Krishna, J.R. Long, Evaluating metal-organic frameworks for post-combustion carbon dioxide capture via temperature swing adsorption, Energy Environ. Sci. 4 (8) (2011) 3030, https://doi.org/10.1039/c1ee01720a.

[10] J. Liu, P.K. Thallapally, B.P. McGrail, D.R. Brown, J. Liu, Progress in adsorption-based CO_2 capture by metal-organic frameworks, Chem. Soc. Rev. 41 (6) (2012) 2308–2322, https://doi.org/10.1039/C1CS15221A.

[11] H. Huang, W. Zhang, F. Yang, B. Wang, Q. Yang, Y. Xie, C. Zhong, J.R. Li, Enhancing CO_2 adsorption and separation ability of Zr(IV)-based metal-organic frameworks through ligand functionalization under the guidance of the quantitative structure-property relationship model, Chem. Eng. J. 289 (2016) 247–253, https://doi.org/10.1016/j.cej.2015.12.100.

[12] M. Sevilla, A.B. Fuertes, Sustainable porous carbons with a superior performance for CO_2 capture, Energy Environ. Sci. 4 (5) (2011) 1765, https://doi.org/10.1039/c0ee00784f.

[13] L. Wang, L. Rao, B. Xia, L. Wang, L. Yue, Y. Liang, H. DaCosta, X. Hu, Highly efficient CO_2 adsorption by nitrogen-doped porous carbons synthesized with low-temperature sodium amide activation, Carbon 130 (2018) 31–40, https://doi.org/10.1016/j.carbon.2018.01.003.

[14] E.S. Sanz-Pérez, T.C. Dantas, A. Arencibia, G. Calleja, A.P. Guedes, A.S. Araujo, R. Sanz, Reuse and recycling of amine-functionalized silica materials for CO_2 adsorption, Chem. Eng. J. 308 (2017) 1021–1033, https://doi.org/10.1016/j.cej.2016.09.109.

[15] R. Sanz, G. Calleja, A. Arencibia, E.S. Sanz-Pérez, CO_2 adsorption on branched polyethyleneimine-impregnated mesoporous silica SBA-15, Appl. Surf. Sci. 256 (17) (2010) 5323–5328, https://doi.org/10.1016/j.apsusc.2009.12.070.

[16] E.R. Monazam, L.J. Shadle, D.C. Miller, H.W. Pennline, D.J. Fauth, J.S. Hoffman, M.L. Gray, Equilibrium and kinetics analysis of carbon dioxide capture using immobilized amine on a mesoporous silica, AIChE J. 59 (3) (2013) 923–935, https://doi.org/10.1002/aic.13870.

[17] F. Liu, K. Huang, C.J. Yoo, C. Okonkwo, D.J. Tao, C.W. Jones, S. Dai, Facilely synthesized meso-macroporous polymer as support of poly(ethyleneimine) for highly efficient and selective capture of CO_2, Chem. Eng. J. 314 (2017) 466–476, https://doi.org/10.1016/j.cej.2016.12.004.

[18] F. Liu, S. Chen, Y. Gao, Synthesis of porous polymer based solid amine adsorbent: Effect of pore size and amine loading on CO_2 adsorption, J. Colloid Interface Sci. 506 (2017) 236–244, https://doi.org/10.1016/j.jcis.2017.07.049.

[19] R. Chatti, A.K. Bansiwal, J.A. Thote, V. Kumar, P. Jadhav, S.K. Lokhande, R.B. Biniwale, N.K. Labhsetwar, S.S. Rayalu, Amine loaded zeolites for carbon dioxide capture: amine loading and adsorption studies, Microporous Mesoporous Mater. 121 (1–3) (2009) 84–89, https://doi.org/10.1016/j.micromeso.2009.01.007.

[20] F. Su, C. Lu, S.C. Kuo, W. Zeng, Adsorption of CO_2 on amine-functionalized y-type zeolites, Energy Fuels 24 (2) (2010) 1441–1448, https://doi.org/10.1021/ef901077k.

[21] M.G. Plaza, C. Pevida, A. Arenillas, F. Rubiera, J.J. Pis, CO_2 capture by adsorption with nitrogen enriched carbons, Fuel 86 (14 SPEC ISS.) (2007) 2204–2212, https://doi.org/10.1016/j.fuel.2007.06.001.

[22] A. Sayari, Y. Belmabkhout, Stabilization of amine-containing CO_2 adsorbents:

dramatic effect of water vapor, J. Am. Chem. Soc. 132 (18) (2010) 6312–6314.
[23] Y. Lin, Q. Yan, C. Kong, L. Chen, Polyethyleneimine incorporated metal-organic frameworks adsorbent for highly selective CO_2 capture, Sci. Rep. 3 (1) (2013) 1859, https://doi.org/10.1038/srep01859.
[24] S. Xian, Y. Wu, J. Wu, X. Wang, J. Xiao, Enhanced dynamic CO_2 adsorption capacity and CO_2/CH_4 selectivity on polyethylenimine-impregnated UiO-66, Ind. Eng. Chem. Res. 54 (44) (2015) 11151–11158, https://doi.org/10.1021/acs.iecr.5b03517.
[25] Y. Belmabkhout, R. Serna-Guerrero, A. Sayari, Adsorption of CO_2-containing gas mixtures over amine-bearing pore-expanded MCM-41 silica: application for CO_2 separation, Adsorption 17 (2) (2011) 395–401, https://doi.org/10.1007/s10450-011-9348-0.
[26] Y. Belmabkhout, A. Sayari, Effect of pore expansion and amine functionalization of mesoporous silica on CO_2 adsorption over a wide range of conditions, Adsorption 15 (3) (2009) 318–328, https://doi.org/10.1007/s10450-009-9185-6.
[27] S. Choi, J.H. Drese, C.W. Jones, Adsorbent materials for carbon dioxide capture from large anthropogenic point sources, ChemSusChem 2 (9) (2009) 796–854, https://doi.org/10.1002/cssc.200900036.
[28] S. Sarkar, P.K. Das, S. Bysakh, Effect of heat treatment on morphology and thermal decomposition kinetics of multiwalled carbon nanotubes, Mater. Chem. Phys. 125 (1–2) (2011) 161–167, https://doi.org/10.1016/j.matchemphys.2010.08.088.
[29] S.K. Smart, A.I. Cassady, G.Q. Lu, D.J. Martin, The biocompatibility of carbon nanotubes, Carbon 44 (6) (2006) 1034–1047, https://doi.org/10.1016/j.carbon.2005.10.011.
[30] Q. Li, C. Liu, X. Wang, S. Fan, Measuring the thermal conductivity of individual carbon nanotubes by the Raman shift method, Nanotechnology 20(14).https://doi.org/10.1088/0957-4484/20/14/145702.
[31] M. Irani, A.T. Jacobson, K.A. Gasem, M. Fan, Modified carbon nanotubes/tetraethylenepentamine for CO_2 capture, Fuel 206 (2017) 10–18, https://doi.org/10.1016/j.fuel.2017.05.087.
[32] F. Rezaei, A. Mosca, P. Webley, J. Hedlund, P. Xiao, Comparison of traditional and structured adsorbents for CO_2 separation by vacuum-swing adsorption, Ind. Eng. Chem. Res. 49 (10) (2010) 4832–4841, https://doi.org/10.1021/ie9016545.
[33] F. Rezaei, P. Webley, Structured adsorbents in gas separation processes, Sep. Purif. Technol. 70 (3) (2010) 243–256, https://doi.org/10.1016/j.seppur.2009.10.004.
[34] X. Feng, C.Y. Pan, C.W. McMinis, J. Ivory, D. Ghosh, Hollow-fiber-based adsorbers for gas separation by pressure-swing adsorption, AIChE J. 44 (7) (1998) 1555–1562, https://doi.org/10.1002/aic.690440709.
[35] R.P. Lively, R.R. Chance, B.T. Kelley, H.W. Deckman, J.H. Drese, C.W. Jones, W.J. Koros, Hollow fiber adsorbents for CO_2 removal from flue gas, Ind. Eng. Chem. Res. 48 (15) (2009) 7314–7324, https://doi.org/10.1021/ie9005244.
[36] R.P. Lively, D.P. Leta, B.A. DeRites, R.R. Chance, W.J. Koros, Hollow fiber adsorbents for CO_2 capture: kinetic sorption performance, Chem. Eng. J. 171 (3) (2011) 801–810, https://doi.org/10.1016/j.cej.2011.01.004.
[37] L. Keller, B. Ohs, J. Lenhart, L. Abduly, P. Blanke, M. Wessling, High capacity polyethylenimine impregnated microtubes made of carbon nanotubes for CO_2 capture, Carbon 126 (2018) 338–345, https://doi.org/10.1016/j.carbon.2017.10.023.
[38] Y. Labreche, R.P. Lively, F. Rezaei, G. Chen, C.W. Jones, W.J. Koros, Post-spinning infusion of poly(ethyleneimine) into polymer/silica hollow fiber sorbents for carbon dioxide capture, Chem. Eng. J. 221 (2013) 166–175, https://doi.org/10.1016/j.cej.2013.01.086.
[39] Y. Fan, Y. Labreche, R.P. Lively, C.W. Jones, W.J. Koros, Dynamic CO_2 adsorption performance of internally cooled silica-supported poly(ethylenimine) hollow fiber sorbents, AIChE J. 60 (11) (2014) 3878–3887, https://doi.org/10.1002/aic.14615.
[40] Y. Fan, J. Kalyanaraman, Y. Labreche, F. Rezaei, R.P. Lively, M.J. Realff, W.J. Koros, C.W. Jones, Y. Kawajiri, CO_2 Sorption performance of composite polymer/amino-silica hollow fiber sorbents: an experimental and modeling study, Ind. Eng. Chem. Res. 54 (6) (2015) 1783–1795, https://doi.org/10.1021/ie504603h.
[41] E.P. Dillon, C.A. Crouse, A.R. Barron, Synthesis, characterization, and carbon dioxide adsorption of covalently attached polyethyleneimine-functionalized single-wall carbon nanotubes, ACS Nano 2 (1) (2008) 156–164, https://doi.org/10.1021/nn7002713.
[42] M.-S. Lee, S.-Y. Lee, S.-J. Park, Preparation and characterization of multi-walled carbon nanotubes impregnated with polyethyleneimine for carbon dioxide capture, Int. J. Hydrogen Energy 40 (8) (2015) 3415–3421, https://doi.org/10.1016/j.ijhydene.2014.12.104.
[43] Z. Zhou, C.M. Anderson, S.K. Butler, S.K. Thompson, K.J. Whitty, T.-C. Shen, K.J. Stowers, Stability and efficiency of CO_2 capture using linear amine polymer modified carbon nanotubes, J. Mater. Chem. A 5 (2017) 10486–10494, https://doi.org/10.1039/C7TA02576A.
[44] Q. Ye, J. Jiang, C. Wang, Y. Liu, H. Pan, Y. Shi, Adsorption of low-concentration carbon dioxide on amine-modified carbon nanotubes at ambient temperature, Energy Fuels 26 (4) (2012) 2497–2504, https://doi.org/10.1021/ef201699w.
[45] Q. Liu, Y. Shi, S. Zheng, L. Ning, Q. Ye, M. Tao, Y. He, Amine-functionalized low-cost industrial grade multi-walled carbon nanotubes for the capture of carbon dioxide, J. Energy Chem. 23 (1) (2014) 111–118, https://doi.org/10.1016/S2095-4956(14)60124-8.
[46] C. Lu, H. Bai, B. Wu, F. Su, J.F. Hwang, Comparative study of CO_2 capture by carbon nanotubes, activated carbons, and zeolites, Energy Fuels 22 (5) (2008) 3050–3056, https://doi.org/10.1021/ef8000086.
[47] F. Su, C. Lu, H.S. Chen, Adsorption, desorption, and thermodynamic studies of CO_2 with high-amine-loaded multiwalled carbon nanotubes, Langmuir 27 (13) (2011) 8090–8098, https://doi.org/10.1021/la201745y.
[48] M.M. Gui, Y.X. Yap, S.P. Chai, A.R. Mohamed, Multi-walled carbon nanotubes modified with (3-aminopropyl)triethoxysilane for effective carbon dioxide adsorption, Int. J. Greenhouse Gas Control 14 (2013) 65–73, https://doi.org/10.1016/j.ijggc.2013.01.004.
[49] H. Hu, T. Zhang, S. Yuan, S. Tang, Functionalization of multi-walled carbon nanotubes with phenylenediamine for enhanced CO_2 adsorption, Adsorption 23 (1) (2017) 73–85.
[50] B. Yang, H. Hu, Q. Yu, X. Zhang, Z. Li, L. Lei, Pretreated multiwalled carbon nanotube adsorbents with amine-grafting for removal of carbon dioxide in confined spaces, RSC Adv. 4 (99) (2014) 56224–56234, https://doi.org/10.1039/C4RA11271G.
[51] W.-J. Son, J.-S. Choi, W.-S. Ahn, Adsorptive removal of carbon dioxide using polyethyleneimine-loaded mesoporous silica materials, Microporous Mesoporous Mater. 113 (1–3) (2008) 31–40, https://doi.org/10.1016/j.micromeso.2007.10.049.
[52] K. Li, J.D. Kress, D.S. Mebane, The mechanism of CO_2 adsorption under dry and humid conditions in mesoporous silica-supported amine sorbents, J. Phys. Chem. C 120 (41) (2016) 23683–23691, https://doi.org/10.1021/acs.jpcc.6b08808.
[53] X. Xu, C. Song, J.M. Andrésen, B.G. Miller, A.W. Scaroni, Preparation and characterization of novel CO_2 molecular basket adsorbents based on polymer-modified mesoporous molecular sieve MCM-41, Microporous Mesoporous Mater. 62 (1–2) (2003) 29–45, https://doi.org/10.1016/S1387-1811(03)00388-3.
[54] B. Dutcher, M. Fan, A.G. Russell, Amine-based CO_2 capture technology development from the beginning of 2013 – a review, ACS Appl. Mater. Interfaces 7 (4) (2015) 2137–2148, https://doi.org/10.1021/am507465f.
[55] Y. Gendel, O. David, M. Wessling, Microtubes made of carbon nanotubes, Carbon 68 (2014) 818–820, https://doi.org/10.1016/j.carbon.2013.11.005.
[56] https://grace.com/coatings-and-inks/en-us/http-grace-com-coatings-and-inks-en-us-matting-agents-portfolio, Grace: SYLOID Matting Agents Characteristics, accessed on April 20, 2018.
[57] X. Xu, C. Song, J.M. Andrésen, B.G. Miller, A.W. Scaroni, Preparation and characterization of novel CO_2 "molecular basket" adsorbents based on polymer-modified mesoporous molecular sieve MCM-41, Microporous Mesoporous Mater. 62 (1–2) (2003) 29–45.
[58] P. de Wit, F.S. van Daalen, N.E. Benes, The mechanical strength of a ceramic porous hollow fiber, J. Membr. Sci. 524 (September 2016) (2017) 721–728, https://doi.org/10.1016/j.memsci.2016.11.047.
[59] A. Arenillas, K.M. Smith, T.C. Drage, C.E. Snape, CO_2 capture using some fly ash-derived carbon materials, Fuel 84 (17) (2005) 2204–2210, https://doi.org/10.1016/j.fuel.2005.04.003.
[60] R.H. Baughman, C. Cui, A.A. Zakhidov, Z. Iqbal, J.N. Barisci, G.M. Spinks, G.G. Wallace, A. Mazzoldi, D. De Rossi, A.G. Rinzler, O. Jaschinski, S. Roth, M. Kertesz, Carbon nanotube actuators, Science 284 (5418) (1999) 1340–1344, https://doi.org/10.1126/science.284.5418.1340.
[61] R. Lively, R.R. Chance, W.J. Koros, H. Deckman, B.T. Kelley, Sorbent fiber compositions and methods of temperature swing adsorption, US Patent 8,133,308, 2012.
[62] F.M. Orr Jr., CO_2 capture and storage: are we ready? Energy Environ. Sci. 2 (5) (2009) 449–458, https://doi.org/10.1039/b822107n.
[63] H. Freundlich, Über die Adsorption in Lösungen, Zeitschrift für Physikalische Chemie 57U (1).https://doi.org/10.1515/zpch-1907-5723.
[64] Y.S. Ho, J.F. Porter, G. McKay, Equilibrium isotherm studies for the sorption of divalent metal ions onto peat: copper, nickel and lead single component systems, Water Air Soil Pollut. 141 (1–4) (2002) 1–33, https://doi.org/10.1023/A:1021304828010.
[65] R. Serna-Guerrero, E. Da'na, A. Sayari, New insights into the interactions of CO_2 with amine-functionalized silica, Ind. Eng. Chem. Res. 47 (23) (2008) 9406–9412, https://doi.org/10.1021/ie801186g.
[66] https://www.esrl.noaa.gov/gmd/ccgg/trends/global.html, ESRL Global Monitoring Division – Global Greenhouse Gas Reference Network, accessed on April 4, 2018.
[67] A.L. Myers, J.M. Prausnitz, Thermodynamics of mixed-gas adsorption, AIChE J. 11 (1) (1965) 121–127, https://doi.org/10.1002/aic.690110125.
[68] Z. Chen, S. Deng, H. Wei, B. Wang, J. Huang, G. Yu, Polyethylenimine-impregnated resin for high CO_2 adsorption: an efficient adsorbent for CO_2 capture from simulated flue gas and ambient air, ACS Appl. Mater. Interfaces 5 (15) (2013) 6937–6945, https://doi.org/10.1021/am400661b.
[69] B. Ohs, M. Krödel, M. Wessling, Adsorption of carbon dioxide on solid amine-functionalized sorbents: a dual kinetic model, Sep. Purif. Technol. 204 (April) (2018) 13–20, https://doi.org/10.1016/j.seppur.2018.04.009.
[70] H. Huang, W. Zhang, D. Liu, B. Liu, G. Chen, C. Zhong, Effect of temperature on gas adsorption and separation in ZIF-8: a combined experimental and molecular simulation study, Chem. Eng. Sci. 66 (23) (2011) 6297–6305, https://doi.org/10.1016/j.ces.2011.09.009.
[71] T.C. Drage, A. Arenillas, K.M. Smith, C.E. Snape, Thermal stability of polyethylenimine based carbon dioxide adsorbents and its influence on selection of regeneration strategies, Microporous Mesoporous Mater. 116 (1–3) (2008) 504–512, https://doi.org/10.1016/j.micromeso.2008.05.009.
[72] W. Li, S. Choi, J.H. Drese, M. Hornbostel, G. Krishnan, P.M. Eisenberger, C.W. Jones, Steam-stripping for regeneration of supported amine-based CO_2 adsorbents, ChemSusChem 3 (8) (2010) 899–903, https://doi.org/10.1002/cssc.201000131.
[73] J. Yu, S.S. Chuang, The role of water in CO_2 capture by amine, Ind. Eng. Chem. Res. 56 (21) (2017) 6337–6347, https://doi.org/10.1021/acs.iecr.7b00715.
[74] A. Heydari-Gorji, Y. Belmabkhout, A. Sayari, Polyethylenimine-impregnated mesoporous silica: Effect of amine loading and surface alkyl chains on CO_2 adsorption, Langmuir 27 (20) (2011) 12411–12416, https://doi.org/10.1021/la202972t.